J Mater Sci (2009) 44:835–842
DOI 10.1007/s10853-008-3120-1

Study of microstructural evolution during static recrystallization in a low alloy steel

Y. C. Lin · Ming-Song Chen

Received: 30 August 2008 / Accepted: 12 November 2008 / Published online: 11 December 2008

Abstract Hot compression tests of 42CrMo steel were carried out on Gleeble-1500 thermo-mechanical simulator. The effects of forming temperature, strain rate, deformation degree, and initial austenite grain size on the microstructural evolution during static recrystallization in hot deformed 42CrMo steel were discussed. Based on the experimental results, the grain size model for static recrystallization was established. It is found that the effects of the processing parameters on the microstructural evolution during static recrystallization are significant, while those of the initial austenitic grain size are not obvious. Additionally, a good agreement between the experimental and predicted grain sizes was also obtained.

Introduction

In industrial forming processes, the hot rolling and forging processes often consist of several successive deformation passes, including inter-pass periods between the deformations. During the inter-pass periods, the metals and alloys will be subjected to dynamic recrystallization [1–3], static recrystallization [4, 5], and metadynamic recrystallization [6, 7]. Meanwhile, the metals and alloys are often subjected to complex time, strain, strain rate, and temperature histories. On the one hand, a given combination of thermo-mechanical parameters yields a particular metallurgical phenomenon (microstructural evolution); on the other hand, microstructural changes of the metal during the hot-forming process in turn affect the mechanical characteristics of the metal such as the flow stress, and hence influences the forming process. In order to achieve the desired mechanical properties of the product, understandings of microstructure changes and softening mechanisms taking place during the complex forming processes, such as multi-stage or multi-pass processing, has a great importance for designers of metal forming processes (hot rolling, forging, and extrusion) because of its effective role on metal flow pattern as well as the kinetics of metallurgical transformation [8–19]. He et al. [8, 9] developed mathematical models to predict the stress–strain curves of this high Nb containing TiAl based alloy during hot deformation. A revised model describing the relationships of the flow stress, strain rate, and temperature of 42CrMo steel at elevated temperatures is proposed by compensation of the strain and strain rate [10]. Lin et al. [11] investigated the static recrystallization kinetics in 42CrMo steel by isothermal double hit hot compression tests and proposed the kinetic equations to predict the softening behaviors induced by static recrystallization. Morris et al. [12] analyzed the strengthening mechanisms in a severely plastically-deformed Al–Mg–Si alloy with submicron grain size. Mandal et al. [13] discussed the kinetics, mechanism, and modelling of the microstructural evolution of a 15Cr–15Ni–2.2Mo–0.3Ti modified austenitic stainless steel (alloy D9) during dynamic recrystallization (DRX), and the kinetics of DRX has been investigated by employing modified Johnson–Mehl–Avrami–Kolmogorov (JMAK) model. Kalaichelvi et al. [15] predicted the flow stress of 6061Al-15% SiC–MMC composites using the conventional regression method, artificial neural network (ANN), and adaptive neuro-fuzzy inference system (ANFIS) method. By comparing the performances of

Y. C. Lin (✉) · M.-S. Chen
Key Laboratory of Modern Complex Equipment Design and Extreme Manufacturing of the Ministry of Education, School of Mechanical and Electrical Engineering, Central South University, Changsha 410083, China
e-mail: yclin@mail.csu.edu.cn; linyongcheng@163.com

various modeling techniques, they found that ANFIS modeling can effectively be employed for the prediction of flow stress of 6061-Al-15% SiCp. Lins et al. [17] characterized the microstructures and texture of a hot-rolled IF steel. Results showed the presence of a diffuse (nearly random) and weak texture in the hot-band that consists of recrystallized polygonal grains and subgrains. Maropoulos et al. [18] examined the effect of varying normalising and hardening temperatures on the prior austenite grain size in a low alloy Cr–Mo–Ni–V steel.

A 42CrMo (American grade: AISI 4140), which is widely used for many general purpose parts, is one of the representative medium carbon and low alloy steel. In the past, many investigations have been carried out on the behaviors of 42CrMo steel [10, 11, 20–22]. Karadeniz [20] studied two different spheroidization processes of AISI 4140 steel in order to improve the properties. Lin et al. [21] established the flow stress constitutive equations, depicting the work hardening-dynamical recovery, and dynamical recrystallization. An artificial neural network (ANN) model was developed to predict the constitutive flow behaviors of 42CrMo steel during single-pass hot deformation [22]. Despite large amount of efforts invested into the behaviors of 42CrMo steel, the microstructural evolutions during static recrystallization in hot deformed 42CrMo steel needs to be further investigated to study the workability and optimize the hot-forming processing parameters.

In this study, the microstructural evolutions during static recrystallization in hot deformed 42CrMo steel were investigated by hot compression tests. The effects of forming temperature, strain rate, deformation degree, and initial austenite grain size on the static recrystallization grain sizes were discussed in details. Based on experimental results, the grain size model for the static recrystallization of 42CrMo steel was established and verified by the experimental results.

Experiments

Materials, specimens, and experimental equipment

A commercial 42CrMo high-strength steel of compositions (wt%) 0.450C–0.280Si–0.960Cr–0.630Mn–0.190Mo –0.016P–0.012S–0.014Cu–(bal.)Fe was used in this investigation. Cylindrical specimens were machined with a diameter of 10 mm and a height of 12 mm. In order to minimize the frictions between the specimens and die during hot deformation, the flat ends of the specimen were recessed to a depth of 0.1 mm to entrap the lubricant of graphite mixed with machine oil. To study the progress of static recrystallization, double hit tests were performed. The hot compression tests were performed on a computer-controlled, servo-hydraulic Gleeble-1500 thermo-simulation machine. It can be programmed to simulate both thermal and mechanical industrial process variables for a wide range of hot deformation conditions. The specimen is resistance heated by thermo coupled-feedback-controlled AC current.

Experimental procedure

As shown in Fig. 1a, the specimens were heated to 1,200 °C at a heating rate of 10 °C/s and held for 5 min. Then, the specimens were cooled to the forming temperature at a rate of 10 °C/s and held for 1 min to eliminate thermal gradients. Three different forming temperatures (850 °C, 950 °C, and 1,050 °C) and four different strain rates (0.1 s^{-1}, 0.5 s^{-1}, 1 s^{-1}, and 2 s^{-1}) were used in hot compression tests. In order to investigate the effects of strain on the microstructural evolution during static recrystallization, four different deformation degrees (a reduction of 5%, 10%, 12%, and 15% in specimen height) were applied. Of course, it should be kept the deformation was interrupted below the critical strain required for dynamic recrystallization. The

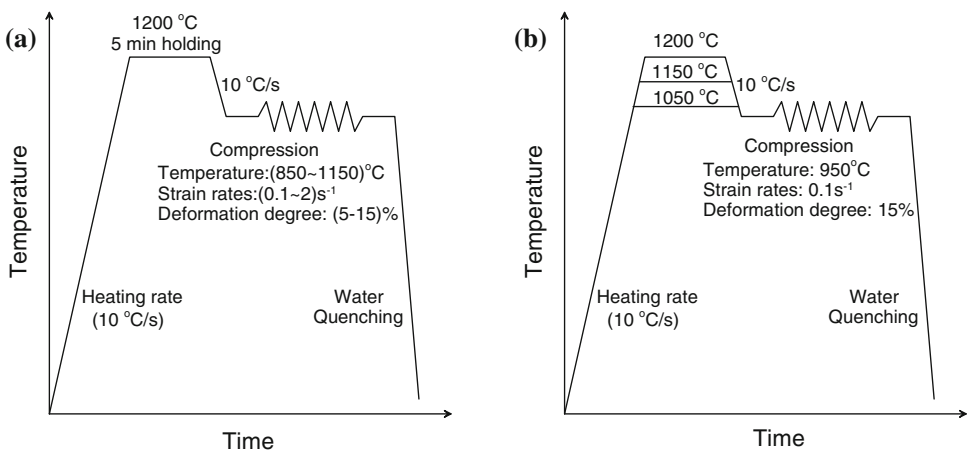

Fig. 1 Experimental procedure for hot compression tests. **a** Considering the effects of processing parameters; and **b** Considering the effects of initial austenite grain size

critical strains had been reported elsewhere [10, 11, 21]. In order to enable full static recrystallization, the specimens were held at the forming temperature for enough time after unloading, and the holding time can be determined from the static recrystallization kinetics reported in the previous publication [11]. Then, the specimens were rapidly quenched in water. Additionally, in order to investigate the effects of initial austenite grain size on the microstructural evolution during static recrystallization, three different heat treatment procedures were used before hot compression, as shown in Fig. 1b. Finally, the deformed blocks were sliced along the axial section. The sections were polished and etched in an abluent solution of saturated picric acid. The optical microstructures in the section plane were examined, as shown in Fig. 2. The grain sizes for the nine positions (from ① to ⑨) at axial section were measured using the method described in the ASTM standards.

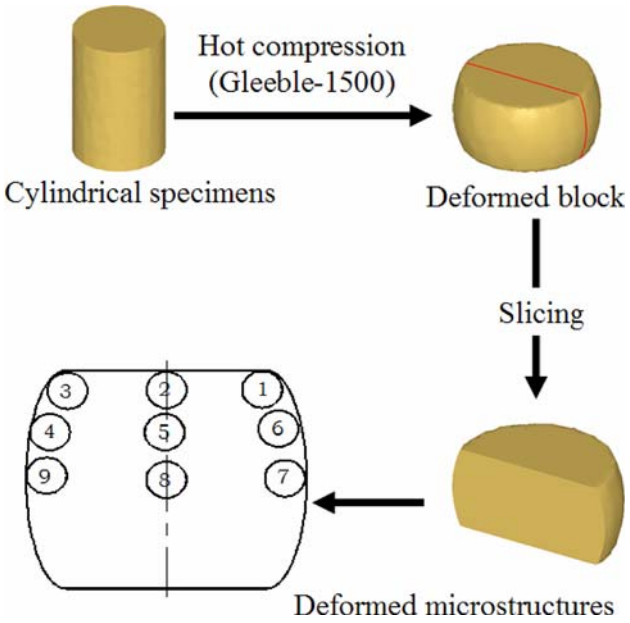

Fig. 2 The nine positions at axial section for optical microstructure analysis

Results and discussion

Influence of the deformation parameters on the static recrystallization grain size

In this section, the effects of deformation parameters, including forming temperature, strain rate, deformation degree, and initial austenite grain size on the microstructural evolution during static recrystallization were discussed in detail.

Effects of forming temperature

The effects of forming temperature on the microstructural evolution during static recrystallization in hot deformed 42CrMo steel were investigated at a deformation degree of

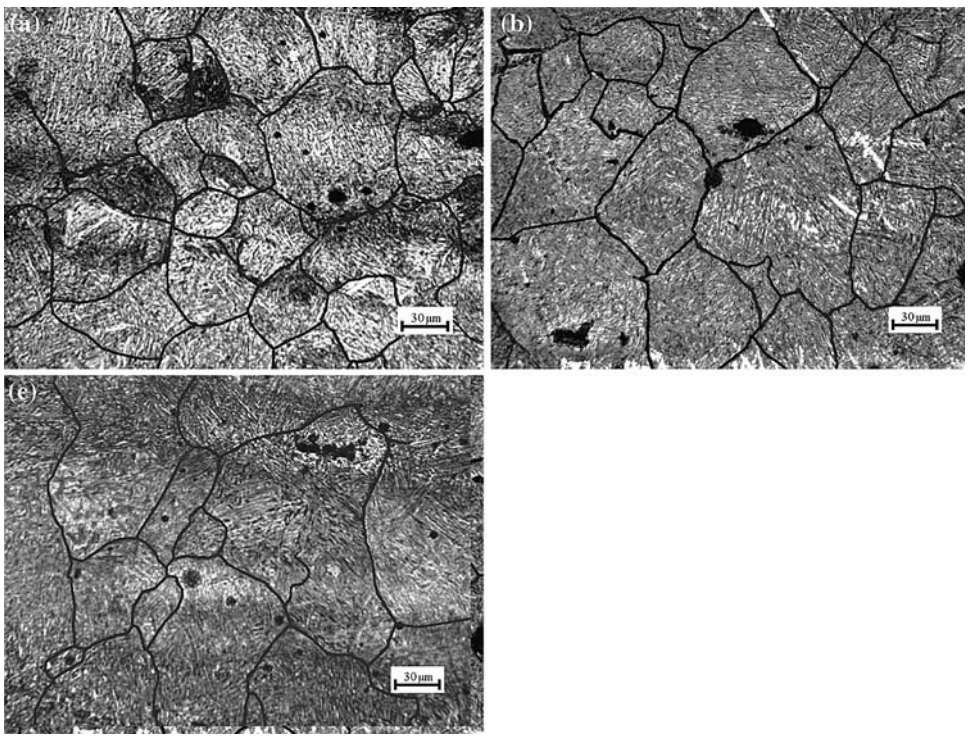

Fig. 3 Optical deformed microstructures of 42CrMo steel (central area of the specimens) after static recrystallization with forming temperatures of **a** 850 °C; **b** 950 °C; and **c** 1,050 °C

15% and strain rate of 0.1 s^{-1}. Figure 3a–c illustrates the optical deformed microstructures at the central area of the section (around the position ⑧) at the temperatures of 850 °C, 950 °C, and 1,050 °C, respectively. It is obvious that the deformed austenite grain size increases with increasing forming temperature. Figure 4 shows the effects of forming temperature on average grain sizes (obtained from the positions ① to ⑨) in deformed 42CrMo steel. The average grain sizes were measured as 46.5 μm, 62.7 μm, and 74.0 μm under the forming temperatures of 850 °C, 950 °C, and 1,050 °C, respectively. The higher the forming temperature, the larger the static recrystallization degree. At a higher forming temperature, grain growth takes place during deformation and larger equiaxed grain structures are obtained. Therefore, the effect of forming temperature on the microstructures of 42CrMo steel is significant.

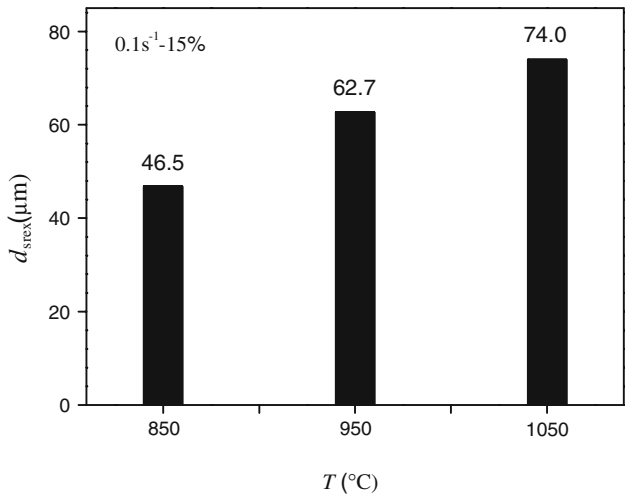

Fig. 4 Effects of forming temperature (T) on the average grain size d_{srex} (obtained from the positions ① to ⑨) in deformed 42CrMo steel after static recrystallization

Effects of strain rate

In this part, the effects of strain rate on the microstructural evolution during the static recrystallization in hot deformed 42CrMo steel were investigated at the deformation degree of 15% and temperature of 1,050 °C. Figure 5a–c shows the optical deformed microstructures at the central area of the section (around the position ⑧) under strain rates of 0.1 s^{-1}, 0.5 s^{-1}, 1 s^{-1}, and 2 s^{-1}, respectively. Figure 6 shows the effects of strain rate on average grain sizes (obtained from the positions ① to ⑨) in deformed 42CrMo steel. It can be easily found that the higher the strain rate, the finer the grains and the average grain sizes were measured as 74.0 μm, 62.5 μm, 57.1 μm, and 52.6 μm under the strain rates of 0.1 s^{-1}, 0.5 s^{-1}, 1 s^{-1}, and 2 s^{-1}, respectively. With the increase of strain rate, dynamic recovery rate decreases. Meanwhile, the dislocation generation rate, the dislocation density, and nucleation sites increase in the deformed microstructure. Then, for the case of high strain rate, there are more deformation energies stored in the deformed blocks. Therefore, it is popular

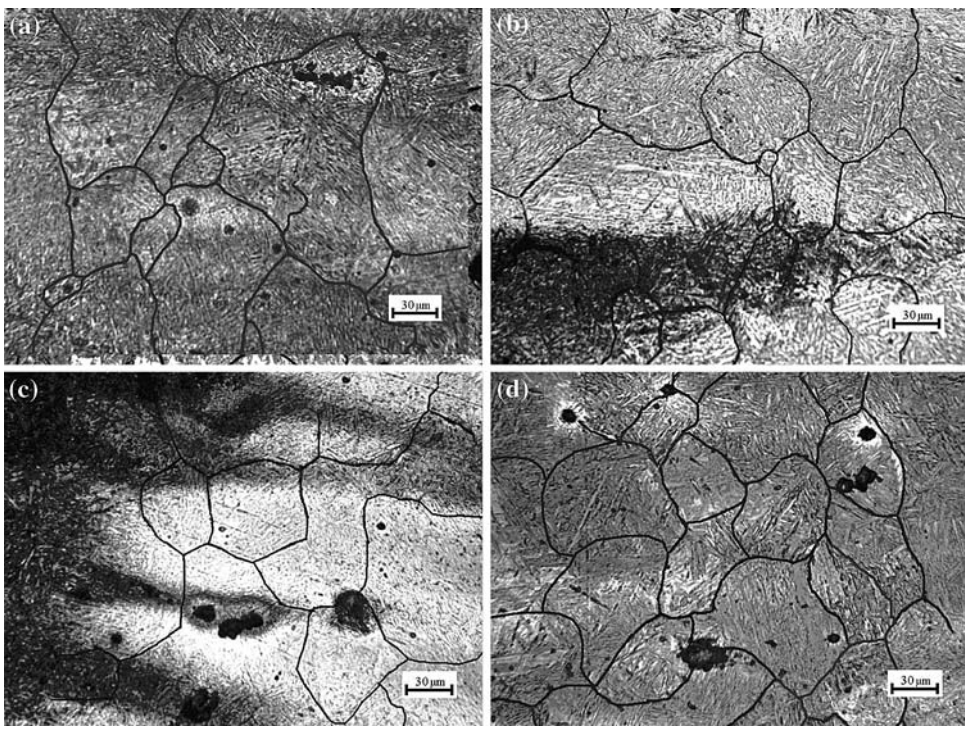

Fig. 5 Optical deformed microstructures of 42CrMo steel (central area of the specimens) after static recrystallization with strain rates of **a** 0.1 s^{-1}; **b** 0.5 s^{-1}; **c** 1 s^{-1}; and **d** 2 s^{-1}

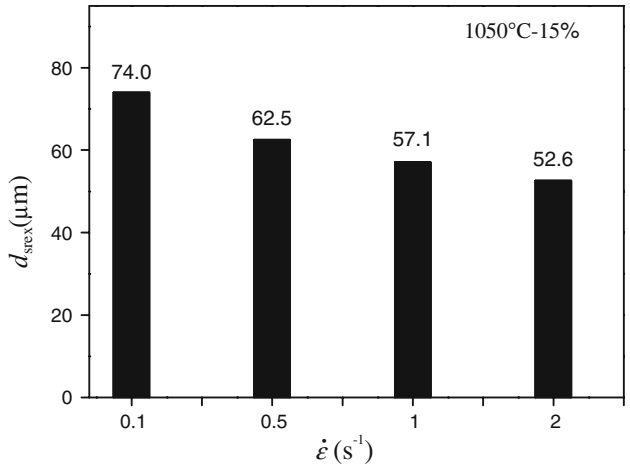

Fig. 6 Effects of strain rates ($\dot{\varepsilon}$) on average grain size d_{srex} (obtained from the positions ① to ⑨) in 42CrMo steel after static recrystallization

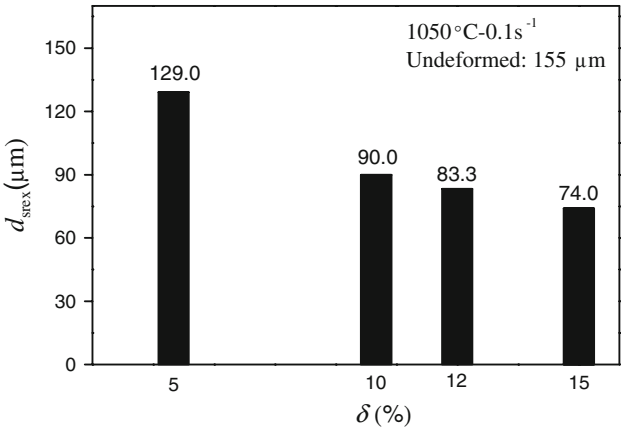

Fig. 8 Effects of deformation degree (δ) on average grain size d_{srex} (obtained from the positions ① to ⑨) in 42CrMo steel after static recrystallization

understood that more substructures can be generated in the initial grains when strain rate is higher, which will produce more nuclei per unit volume of the grains. This mechanism can make the grain finer when strain rate is higher. When the strain rate is decreased, the dynamic recovery rate increases and the dynamic recovery proceeds adequately during deformation. So, the grain sizes under lower strain rate are larger than those under higher strain rate. Therefore, the effects of strain rate on the microstructural evolution during static recrystallization in hot deformed 42CrMo steel are significant.

Effects of deformation degree

In this part, the effects of deformation degree, i.e., a reduction in specimen height, on the microstructural evolution during static recrystallization in hot deformed 42CrMo steel was investigated under the strain rate of 0.1 s^{-1} and forming temperature of 1,050 °C. The optical microstructures at the central area of the section (around the position ⑧) of 42CrMo steel with deformation degree of 0 (underformed), 5%, 10%, and 12% are shown in Fig. 7a–d, respectively. Figure 8 shows the effects of deformation

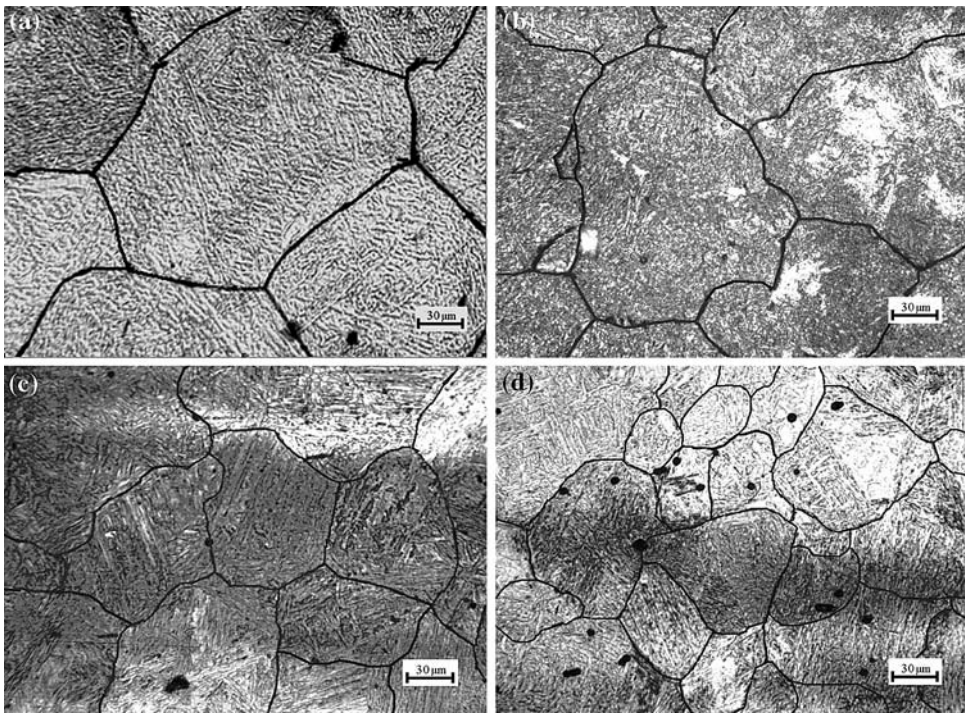

Fig. 7 Optical deformed microstructures of 42CrMo steel (central area of the specimens) after the static recrystallization with deformation degrees of **a** underformed; **b** 5%; **c** 10%; and **d** 12%

degree on average grain sizes (obtained from the positions ① to ⑨) in deformed 42CrMo steel. Additionally, the grain size in Fig. 7d seems inhomogeneous, which may be induced by the different orientation of the grain size. When calculating the average grain sizes, which were used to develop the grain size mode during static recrystallization, the inhomogeneous parts can be not considered. Therefore, a little inhomogeneous distribution in certain areas may not pose great effects on the accuracy of the grain size model. The microstructure before compression test has an equiaxed grain structure with an average grain size of about 155 μm, while the average grain sizes for the deformed structures were measured as 129.0 μm, 90.0 μm, 83.3 μm, and 74.0 μm for the deformation degree of 5%, 10%, 12%, and 15% cases, respectively. The higher the deformation degree, the finer the grains. When the deformation degree is large, the dislocation generation rate, the dislocation density, and deformation energy stored in the deformed structures all increases. So, for the larger deformation degree, the recrystallized grains nucleate more easily, which may result in that the grains become finer and the grain boundary area per unit volume increases. Hence, during large strain deformation of metals and alloys the structural changes are characterized by the formation of strain-induced dislocation subboundaries, such as subgrain walls, shearbands, microbands and dense dislocation walls, resulting in continuous subdivision of coarse grains into misoriented fine domains.

Effects of initial grain sizes

Figure 9a–c shows the optical microstructures at the central area of the section (around the position ⑧) of hot deformed 42CrMo steel with different initial austenitic grain sizes (under the strain rate of 0.1 s^{-1}, deformation degree of 15%, and forming temperature of 950 °C). Figure 10 shows the effects of initial austenitic grain size on average grain sizes (obtained from the positions

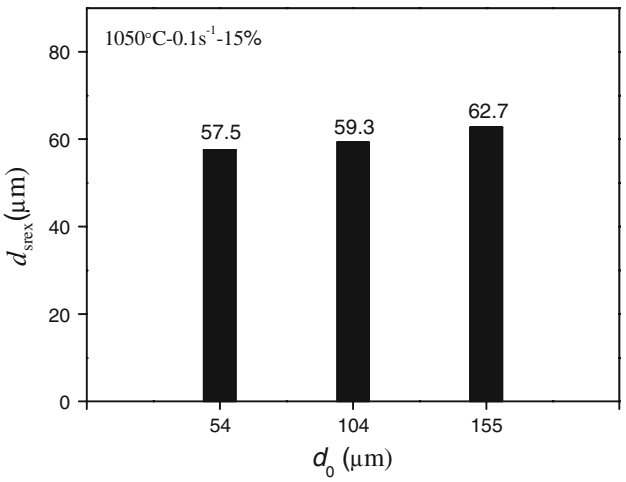

Fig. 10 Effects of initial austenitic grain size (d_0) on average grain size d_{srex} (obtained from the positions ① to ⑨) in 42CrMo steel after static recrystallization

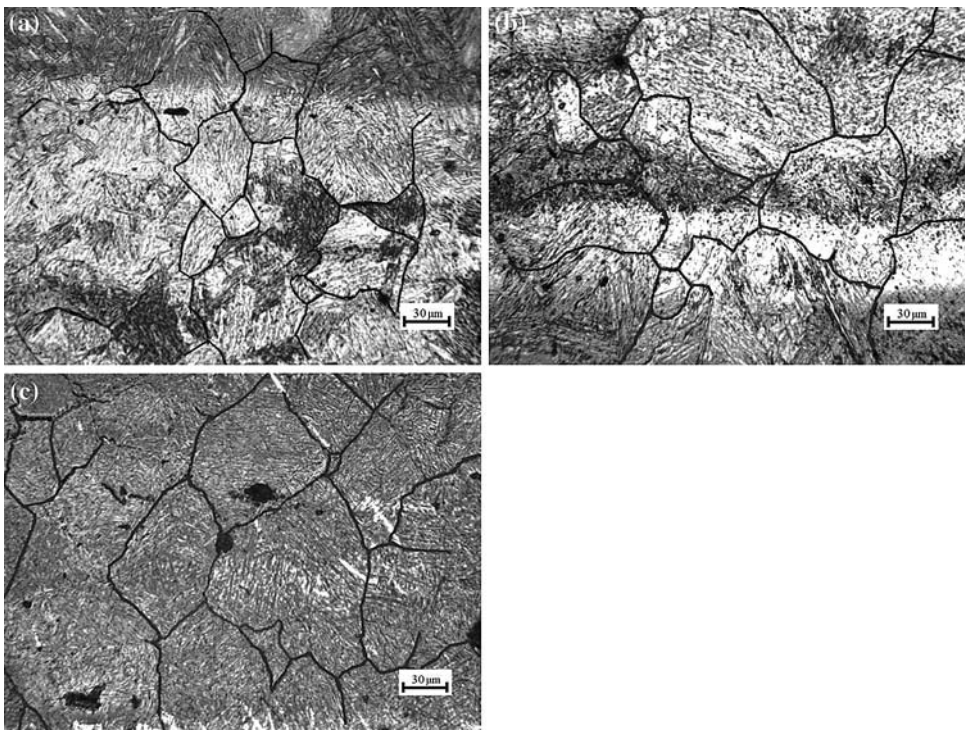

Fig. 9 Optical deformed microstructures of 42CrMo steel (central area of the specimens) after static recrystallization with initial austenitic grain sizes of **a** 54 μm; **b** 104 μm; and **c** 155 μm

① to ⑨). It is obvious that the final grain sizes increase as the initial austenitic grain sizes increase. However, it is not very markable. So, the effect of initial austenitic grain sizes on the microstructural evolutions during static recrystallization in hot deformed 42CrMo steel is not significant.

Grain size model for the static recrystallization

Based on the above experimental results and analysis, the forming temperature, strain rate, deformation degree, and initial austenite grain size will affect the microstructural evolutions during static recrystallization in hot-forming process. The static recrystallization grain size (d_{srex}) can be expressed as a function of forming temperature, strain rate, deformation degree, and initial austenite grain size [23, 24].

$$d_{srex} = a d_0^h \varepsilon^n \dot{\varepsilon}^m \exp[-Q/(RT)] \quad (1)$$

where a, h, n, and m are material dependent constants, d_0 is the initial austenite grain size (μm), ε is the true strain, $\dot{\varepsilon}$ is the strain rate, R is the gas constant (J/mol K), T is the absolute temperature (K), and Q is the apparent activation energy of static recrystallization (kJ/mol).

Taking the logarithm of both sides of Eq. 1 gives,

$$\ln d_{srex} = \ln a + h \ln d_0 + n \ln \varepsilon + m \ln \dot{\varepsilon} - Q/(RT) \quad (2)$$

By substituting the values of static recrystallization grain sizes (d_{srex}) and forming temperatures, static recrystallization grain sizes (d_{srex}) and strain rates, static recrystallization grain sizes (d_{srex}) and true strain, and static recrystallization grain sizes (d_{srex}) and initial grain sizes (d_0) into Eq. 2, respectively, the relationships $1/T - \ln d_{srex}$, $\ln \dot{\varepsilon} - \ln d_{srex}$, $\ln \varepsilon - \ln d_{srex}$, and $\ln d_0 - \ln d_{srex}$ can be obtained as shown in Fig. 11a–d, respectively. From these figures, it is easy to evaluate the values of material dependent constant a, h, n, and m as 215.6, 0.078, −0.48, and −0.114, respectively. The apparent activation energy of static recrystallization (Q) is also obtained as 284.48 kJ/mol.

Then, the grain size model for static recrystallization of 42CrMo steel can be represented as the following equations:

$$d_{srex} = 215.6 d_0^{0.078} \varepsilon^{-0.48} \dot{\varepsilon}^{-0.114} \exp[-28448/(RT)] \quad (3)$$

Comparison between the experimental and predicted results

In order to verify the above-developed grain size model for static recrystallization of hot deformed 42CrMo steel, Eq. 3, comparisons between the experimental and predicted results were carried out. Of course, the dataset used to develop the grain size model were not used again here. Figure 12 shows the comparisons between the experimental and predicted grain size after static recrystallization. It can be found that the predicted results are in good agreement with the experimental ones, which indicates that

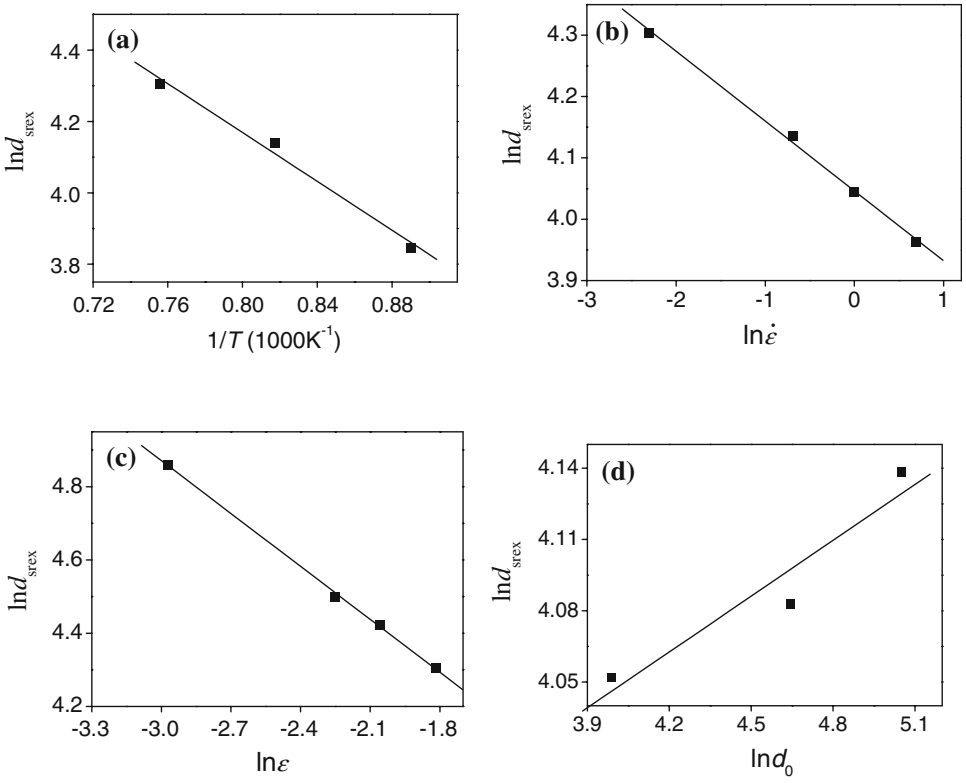

Fig. 11 Relationship between processing parameters and austenitic grain size in 42CrMo steel after the static recrystallization:
a $1/T - \ln d_{srex}$;
b $\ln \dot{\varepsilon} - \ln d_{srex}$;
c $\ln \varepsilon - \ln d_{srex}$; and
d $\ln d_0 - \ln d_{srex}$

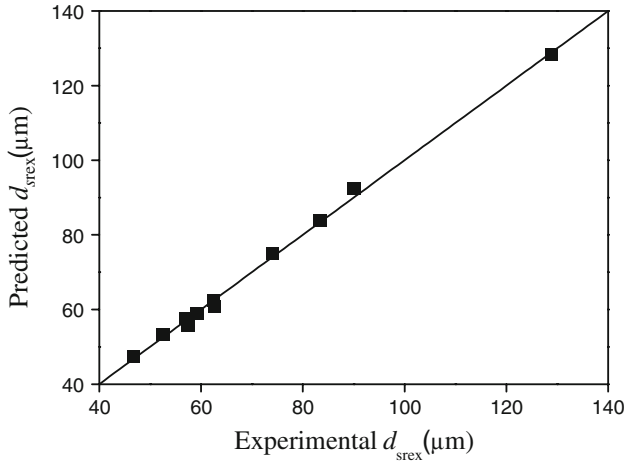

Fig. 12 Comparisons between the experimental and predicted austenitic grain sizes after static recrystallization

the developed grain size model can give an accurate and precise estimate of microstructural evolutions during static recrystallization for hot deformed 42CrMo steel, and can be used to analyze the problems during metal forming process.

Conclusions

In this study, hot compression tests of 42CrMo steel were carried out on Gleeble-1500 thermo-mechanical simulator in order to study the workability and optimize hot formation processing parameters for 42CrMo steel. The effects of forming temperature, strain rate, deformation degree, and initial austenite grain size on the microstructural evolution during static recrystallization in hot deformed 42CrMo steel were investigated by metallurgical analysis. The grain size model for static recrystallization was developed based on the experimental results. It has been found that the processing parameters significantly affect the microstructural evolution during static recrystallization. The deformed austenite grain size increases with the increase in the forming temperature and the decrease in the strain rate. The higher the deformation degree, the finer the grains. However, the effect of initial austenitic grain sizes on the microstructural evolutions during static recrystallization is not significant. A good agreement between the experimental and predicted results indicates that the developed grain size model for static recrystallization can give an accurate and precise estimate of microstructural evolutions for 42CrMo steel, and can be used to analyze the problems during metal forming process.

Acknowledgement This work was supported by 973 Program (Grant No.2006CB705401), National Natural Science Foundation of China (No. 50805147), China Postdoctoral Science Foundation (Grant No.20070410302), and the Postdoctoral Science Foundation of Central South University.

References

1. Hakamada M, Watazu A, Saito N, Iwasaki H (2008) J Mater Sci 43:2066. doi:10.1007/s10853-008-2474-8
2. Mandal S, Sivaprasad PV, Dube RK (2007) J Mater Eng Perform 16:672. doi:10.1007/s11665-007-9098-z
3. Dehghan-Manshadi A, Hodgson PD (2008) J Mater Sci 43:6272. doi:10.1007/s10853-008-2907-4
4. Fernández AI, Uranga P, López B, Rodriguez-ibabe JM (2000) ISIJ Int 40:893
5. Poliak EI, Jonas JJ (2004) ISIJ Int 44:1874
6. Elwazri AM, Essadiqi E, Yue S (2004) ISIJ Int 44:744
7. Lin YC, Fang XL, Wang YP (2008) J Mater Sci 43:5508. doi:10.1007/s10853-008-2832-6
8. He XM, Yu ZQ, Liu GM, Wang WG, Lai XM (2009) Mater Des 30:166. doi:10.1016/j.matdes.2008.04.046
9. He XM, Yu ZQ, Lai XM (2008) Mater Lett 62:4181. doi:10.1016/j.matlet.2008.05.071
10. Lin YC, Chen MS, Zhong J (2008) Comput Mater Sci 42:470. doi:10.1016/j.commatsci.2007.08.011
11. Lin YC, Chen MS, Zhong J (2008) Comput Mater Sci 44:316. doi:10.1016/j.commatsci.2008.03.027
12. Morris DG, Gutierrez-Urrutia I, Muñoz-Morris MA (2007) J Mater Sci 42:1439. doi: 10.1007/s10853-006-0564-z
13. Mandal S, Sivaprasad PV, Dube RK (2007) J Mater Sci 42:2724. doi:10.1007/s10853-006-1275-1
14. Xu LJ, Xing JD, Wei SZ, Peng T, Zhang YZ, Long R (2007) J Mater Sci 42:2565. doi: 10.1007/s10853-006-1278-y
15. Kalaichelvi V, Sivakumar D, Karthikeyan R, Palanikumar K (2008) Mater Des. doi: 10.1016/j.matdes.2008.06.022
16. Garcia-Mateo C, Capdevila C, Caballero FG, García de Andrés C (2007) J Mater Sci 42:5391. doi: 10.1007/s10853-006-0881-2
17. Lins JFC, Sandim HRZ, Kestenbach HJ (2007) J Mater Sci 42:6572. doi:10.1007/s10853-007-1515-z
18. Maropoulos S, Karagiannis S, Ridley N (2007) J Mater Sci 42:1309. doi:10.1007/s10853-006-1191-4
19. Saha R, Ray RK (2008) J Mater Sci 43:207. doi: 10.1007/s10853-007-2139-z
20. Karadeniz E (2008) Mater Des 29:251
21. Lin YC, Chen MS, Zhong J (2008) Mech Res Commun 35:142. doi:10.1016/j.mechrescom.2007.10.002
22. Lin YC, Zhang J, Zhong J (2008) Comput Mater Sci 43:752. doi:10.1016/j.commatsci.2008.01.039
23. Phaniraj MP, Behera BB, Lahiri AK (2006) J Mater Process Technol 178:388
24. Nakata N, Militzer M (2005) ISIJ Int 45:82